Jurnal Teknologi
Full paper

Synthesis and Luminescence Properties of Doped Magnesium Boro-Tellurite Ceramics

Nur Zu Ira Bohari[a],* R. Hussin[a], Zuhairi Ibrahim[a], Hendrik O. Lintang[b]

[a]Phosphor Research Group, Department of Physics, Faculty of Science, *Universiti Teknologi Malaysia, 81310 UTM Johor Bahru, Johor Malaysia*
[b]*Ibnu Sina Institute for Fundamental Science Studies, Universiti Teknologi Malaysia, 81310 UTM Johor Bahru, Johor Malaysia*

*Corresponding author: nzuira@gmail.com

Article history

Received: 05 July 2014
Received in revised form:
17 November 2014
Accepted: 1 February 2015

Graphical abstract

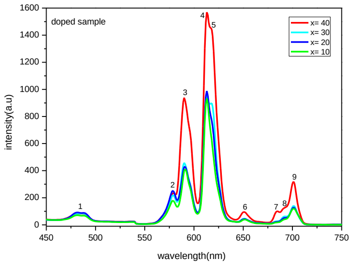

Abstract

Glass has been widely utilized in the field of lighting, telecommunication and spectroscopy. Boro-tellurite is one of the suitable glasses used for solid state lighting and laser application. The investigation on the luminescence properties of rare earth doped ceramic is rarely used due to the opacity. In this paper boro-tellurite prepared in ceramic can show the better luminescence with the less advantage. The aim of this paper is to present the effect and advantages in luminescence results of boro-tellurite ceramics doped with the constant amount of rare earth. Doped magnesium boro-tellurite with Eu^{3+} and Dy^{3+} ceramic have been prepared using solid state reaction method with the compositions of $x\mathrm{TeO_2}$-$(70-x)\mathrm{B_2O_3}$-30MgO with $10 \leq x \leq 40$, and have been doped with Eu_2O_3 (1mol%) and Dy_2O_3 (1mol%) . The characterizations of the samples have been investigated by means of X-Ray diffraction, Raman, Infrared and Photoluminescence spectroscopy. From the X-ray diffraction results, two phases are assigned to $MgTe_2O_5$ and $Mg_2B_2O_5$. Raman spectroscopy showed strong bands observed in the vicinity of 140, 175, 220, 266, 332, 403, 436, 646, 694, 723, 757 and 806 cm^{-1}. FTIR spectra showed bands located in the range between 400-800 cm^{-1} are assigned to the bending mode of Te-O-Te, TeO_3 and TeO_4. In the range of 800-1400 cm^{-1}, the bands are associated with B-O, B-O-B, BO_3 and BO_4 bonds. The emission transition $^5D_0$-$^7F_2$ corresponded to the red emission (612 nm) was found to be the most intense in all the Eu^{3+}-doped magnesium boro-tellurite ceramics.

Keywords: Magnesium boro-tellurite ceramic, luminescence, doped Eu^{3+} and Dy^{3+}

Abstrak

Kaca telah digunakan secara meluas dalam bidang pencahayaan, telekomunikasi dan spektroskopi. Boro-tellurite adalah satu kaca yang sesuai digunakan dalam pencahayaan keadaan pepejal dan aplikasi laser. Penyelidikan luminesens bagi nadir bumi dop seramik adalah jarang digunakan disebabkan oleh kelegapan. Dalam kertas ini boro-tellurite seramik menunjukkan luminesens yang baik dengan kelebihan kurang. Matlamat kertas ini adalah untuk menunjukkan kesan dan kelebihan dalam keputusan luminesens bagi seramik boro-tellurite dop dengan amaun nadir bumi yang tetap. Dop magnesium boro-tellurite dengan Eu^{3+} and Dy^{3+} seramik disediakan dengan menggunakan kaedah tindakbalas keadaan pepejal yang berkomposisi $x\mathrm{TeO_2}$-$(70-x)\mathrm{B_2O_3}$-30MgO dengan $10 \leq x \leq 40$, dan dop Eu_2O_3 (1mol%) and Dy_2O_3 (1mol%). Pencirian sampel disiasat oleh spektroskopi pembelauan sinar-X, Raman, infra merah and Fotoluminesens. Dari keputusan XRD, dua fasa dilihat sebagai $MgTe_2O_5$ and $Mg_2B_2O_5$. Spektroskopi Raman menunjukkan jalur kuat dilihat sekitar 140, 175, 220, 266, 332, 403, 436, 646, 694, 723, 757 dan 806 cm^{-1}. Spektra FTIR menunjukkan jalur terletak dalam lingkungan 400-800 cm^{-1} adalah mod lentur bagi Te-O-Te, TeO_3 and TeO_4. Dalam lingkungan 800-1400 cm^{-1}, jalur yang berkaitan adalah B-O, B-O-B, BO_3 and BO_4. Peralihan pancaran $^5D_0$-$^7F_2$ yang merujuk kepada pancaran merah (612 nm) didapati menjadi yang paling tinggi dalam semua seramik Eu^{3+}-dop magnesium boro-tellurite.

Kata kunci: Seramik magnesium boro-tellurite, luminesens, dop Eu^{3+} and Dy^{3+}

■1.0 INTRODUCTION

Ceramic based on boro-tellurite host matrices doped with rare earth have tremendous applications for lasers, optical amplifier, photo sensitivity, optical storage, and bio-ceramics materials [1-8]. Currently, a great deal of research has been focused on rare earth (RE) doped glasses owing to their extensive applications [9-10]. But, the investigation on the luminescence properties of rare earth doped ceramic is rarely used due to the opacity and hence, limited their applications. Eu^{3+} ion doped sodium-aluminum-tellurite (Eu^{3+}: NAT) was prepared in opaque ceramics compound [11].

The host material with low phonon energy that can reduce the non-radiative loss, play important role for obtaining highly efficient luminescent properties via multiphonon relaxations and thus achieve strong luminescence [12]. In this study, tellurite oxide based has been utilized due to their desirable physical properties, such as high refractive index, excellent infrared transmittance and high dielectric constant, good chemical durability and low melting temperature. On the other hand, borate has important physical properties such as high transparency, low melting point, high thermal stability, good rare earth ions solubility, resistance to chemicals and can enhance mechanical durability [3]. Addition of alkali oxide (MgO) as network modifier has also been employed since the utilization of modifier doped with boro-tellurite based are rarely reported.

The aim of this work is to prepare doped magnesium boro-tellurite ceramics via solid state reaction route and to study the behavior through X-Ray Diffraction (XRD), Infrared (IR), Raman and Photoluminescence (PL) spectroscopic for both materials. The concentration of Eu^{3+} and Dy^{3+} will remain constant.

■2.0 EXPERIMENTAL

High purity of H_3BO_3 (99.99%), TeO_2 (99.99%), MgO (99.99%), Eu_2O_3 (99.99%) and Dy_2O_3 (99.99%) were used as the raw materials. Two types of sample were prepared for the study; magnesium boro-tellurite ceramic and magnesium boro-tellurite with Eu^{3+} and Dy^{3+} ceramic. The samples with the compositions of $x TeO_2$-$(70-x)B_2O_3$-30MgO with $10 \leq x \leq 40$ mol%, doped with Eu_2O_3(1mol%) and Dy_2O_3(1mol%) have been prepared using solid state reaction method. Analytical grade reagents of H_3BO_3, TeO_2, MgO, Eu_2O_3 and Dy_2O_3 powders in appropriate amounts (mol%) were thoroughly mixed in agate mortar. The mixtures were pressed into pellets using hydraulic press with 10 ton/cm^2 of pressure. Pelletized samples were then heat treated at 650 °C for 6 hours. The dried pellet was grounded into fine powder for further characterizations.

Several experiments have been setup to determine the physical nature and characteristics of the prepared samples. The examination of the structure was examined using X-ray diffraction (XRD) using Siemen Diffraction D500 diffractometer with CuKα radiation [13]. Fourier transform infrared spectroscopy (FTIR) was examined using Perkin-Elmer spectrometer (Spectrum 100) [13]. Raman spectroscopy was examined using Bruker model RFS 100/S FT-Raman spectrometer. The emission spectra were obtained using Jasco Fluorescence spectrophotometer, Model FP8000 series, at room temperature.

■3.0 RESULTS AND DISCUSSION

X-ray diffraction technique was used to identify the crystalline phase of the doped magnesium boro-tellurite with Eu^{3+} and Dy^{3+} ceramics. The XRD patterns, Figure 1, show the influence of varying composition of the $xTeO_2$-$(70-x)B_2O_3$-30MgO with $10 \leq x \leq 40$ mol%. The x-ray diffractogram showed well-defined peaks which indicate the crystalline and phase formation of the synthesized compounds. There are two main phases; namely $MgTe_2O_5$ (ICDD: 01-073-3922) and $Mg_2B_2O_5$ (ICDD: 01-073-2107). The intensity increased with B_2O_3 and decrease with TeO_2, ranging from x = 10 to 40. $MgTe_2O_5$ became a dominant phase in the sample followed by $Mg_2B_2O_5$ phase. The majority phase of $MgTe_2O_5$ is an evident that the TeO_2 contribute to the formation of the phase. The percentage of the crystalline phase can be estimated by comparing the highest peak heights summarized in the Table 1. From the estimation of Table 1, it can be concluded that the $MgTe_2O_5$ was the dominant phase.

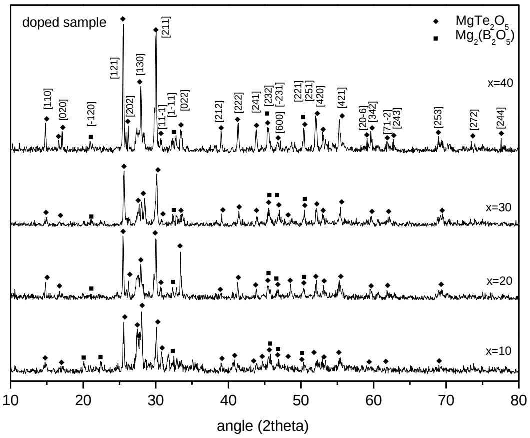

Figure 1 X-ray diffraction pattern of $x TeO_2$-$(70-x)B_2O_3$-30MgO doped Eu^{3+} and Dy^{3+} ceramic ($10 \leq x \leq 40$ mol%)

Table 1 The estimation of percentage of the crystalline phase of xTeO2-$(70-x)B_2O_3$-30MgO doped Eu^{3+} and Dy^{3+} ceramic ($10 \leq x \leq 40$ mol%)

x	$MgTe_2O_5$ phase (%)	$Mg_2B_2O_5$ phase (%)
10	58.03	41.97
20	62.94	37.05
30	67.94	32.06
40	76.00	23.99

Raman spectrum of $x TeO_2$-$(70-x)B_2O_3$-30MgO are presented in Figure 2. Raman spectroscopy show the strong band are observed at 140, 175, 220, 266, 332, 403, 436, 646, 694, 723, 757 and 806 cm^{-1}. Raman spectrum shows that besides the expected TeO_4, Te-O-Te, and BO_3 (peak 7 to 12) existent, the vibrations corresponding to the metal ions are also present in ceramics (peak 1 to 6), respectively.

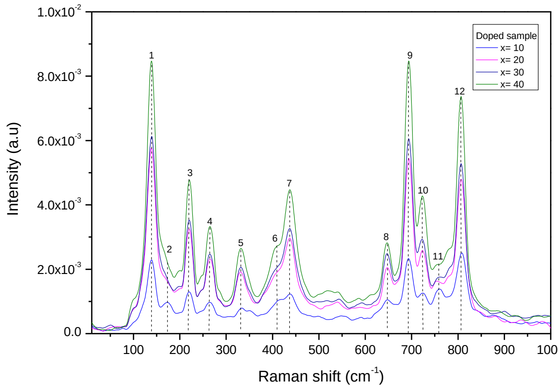

Figure 2 Raman spectra of $x TeO_2$-$(70-x)B_2O_3$-30MgO doped Eu^{3+} and Dy^{3+} ceramic ($10 \leq x \leq 40$ mol%)

The infrared spectrum of xTeO$_2$-(70-x)B$_2$O$_3$-30MgO with 10≤x≤40 mol% in the range 1400-4000cm^{-1} are presented in the Figure 3. There are four bands in this range when the peaks represent OH- and H- units are at around 3215 cm^{-1}, 2920 cm^{-1} and 2261 cm^{-1}. The peaks observed between 3375 cm^{-1} and 4000 cm^{-1} are the hydroxyl groups due to OH- stretching and the peaks observed between (2800-2900) cm^{-1} are the hydrogen bond [9]. Based on the Figure 3, the peaks around 1500 cm^{-1} are due to the B-O stretching of BO$_3$ units which are observed and the band became smaller (x=40), indicating a decrease in TeO$_2$ amounts and increasing B$_2$O$_3$.

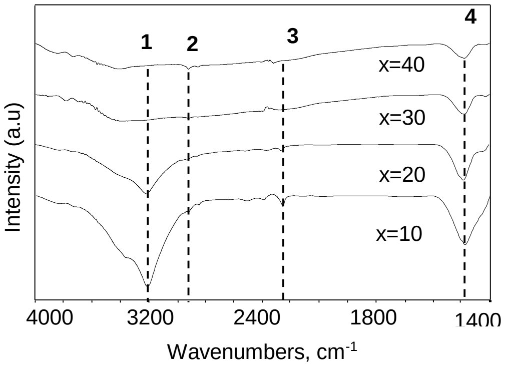

Figure 3 IR spectra of xTeO$_2$-(70-x)B$_2$O$_3$-30MgO doped Eu^{3+} and Dy^{3+} ceramic (10≤x≤40 mol%)

In Figure 4, the IR spectra of xTeO$_2$-(70-x)B$_2$O$_3$-30MgO with 10≤x≤40 mol% in the range (800-1400) cm^{-1} is presented. The bands located in the range between (400-800) cm^{-1} are assigned to the bending mode of Te-O-Te, TeO$_3$ and TeO$_4$. In the range of (800-1400) cm^{-1}, the B-O bond of B-O-B, BO$_3$ and BO$_4$ also appeared. The bands located around (1331-1362) cm^{-1} are assigned to BO$_3$ units [15, 21] and in the range between (881-1200) cm^{-1} which is the BO$_4$ units [10, 14, 16]. The bands positions around 431 cm^{-1}-564 cm^{-1}, 610-680 cm^{-1} and 700- 780 cm^{-1} showed the Te-O-Te, TeO$_2$ and TeO$_3$ respectively. All of these assignments are in good agreement with the reported literature [10, 17-18]. In Figure 4, the band gradually increased with TeO$_2$. The intensity of the band in the range of 431-780 cm^{-1} increased gradually with TeO$_2$ and the intensity of the band slightly decreased with B$_2$O$_3$ in the range of 881-1362 cm^{-1}.

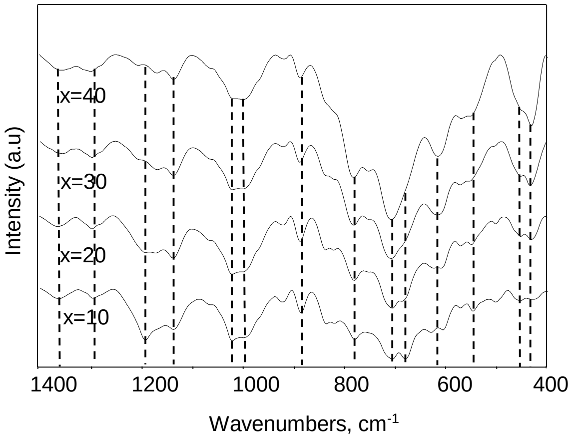

Figure 4 IR spectra of xTeO$_2$-(70-x)B$_2$O$_3$-30MgO doped Eu^{3+} and Dy^{3+} ceramic (10≤x≤40 mol%)

The emission spectrum of doped xTeO$_2$-(70-x)B$_2$O$_3$-30MgO with 10≤x≤40 mol% is shown in Figure 5. The emission transitions $^5D_0 \rightarrow {}^7F_0$, $^5D_0 \rightarrow {}^7F_0$, $^5D_0 \rightarrow {}^7F_1$, $^5D_0 \rightarrow {}^7F_2$, $^5D_0 \rightarrow {}^7F_2$, $^5D_0 \rightarrow {}^7F_3$, $^5D_0 \rightarrow {}^7F_4$, $^5D_0 \rightarrow {}^7F_4$ and $^5D_0 \rightarrow {}^7F_4$ corresponded to the band position at 484.58, 578.17, 589.89, 612.82, 618.38, 651.23, 683.48, 691.53 and 700.85 nm, respectively. It can be noted that a series of Eu^{3+} characteristic emission lines are between 540 nm and 780 nm, which includes the most prominent peak at 612 nm and corresponding to the $^5D_0 \rightarrow {}^7F_J$ (J=0, 1, 2, 3, 4) transitions [19]. The luminescence spectrum was found to be lowest for the sample x = 10 followed by x = 20, 30 and 40. The $^5D_0 \rightarrow {}^7F_2$ transition is more intense than the other transitions as reported in the other literatures [20-22].

The emission peaks of Dy^{3+} were observed at 484.58 nm and 578.17 nm (peak 1 and 2) similar with the other reported values [23]. Figure 5 shows the emission peaks of Eu^{3+} are more dominant with high intensity compared the peaks of Dy^{3+}. The Dy^{3+} emission peaks are not present as dominant peak which indicates that Dy^{3+} acts as trap centers that cause long afterglow characteristics, rather than the luminescent centers in the host lattice [24].

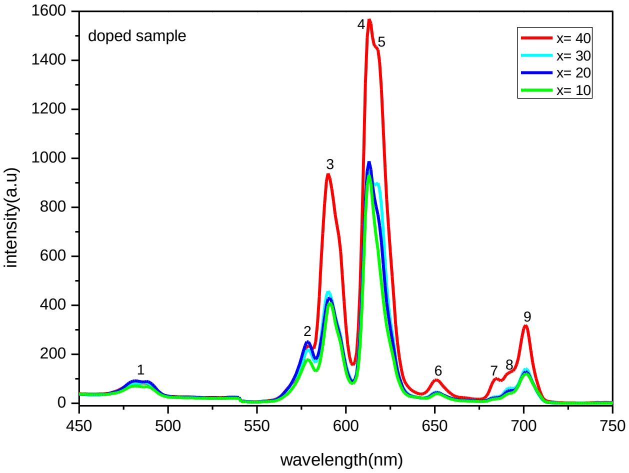

Figure 5 Emission spectrum of xTeO$_2$-(70-x)B$_2$O$_3$-30MgO doped Eu^{3+} and Dy^{3+} ceramic (10≤x≤40 mol%)

■4.0 CONCLUSION

The samples of xTeO$_2$-(70-x)B$_2$O$_3$-30MgO with 10≤x≤40 mol% doped with Eu$_2$O$_3$(1mol%) and Dy$_2$O$_3$(1mol%) have been prepared using solid state route. The structural studies of the samples have been investigated using X-ray diffraction (XRD), Infrared and Raman spectroscopy. The XRD profiles show that MgTe$_2$O$_5$ became a dominant phase in the sample followed by Mg$_2$B$_2$O$_5$ phase. The IR spectrum shows two series of band regions which obtained in 4000-1400cm^{-1} and the second region of 1400-400cm^{-1}. The ceramics doped with Eu^{3+} shows a bright red emission at 612nm which belongs to the electric dipole ($^5D_0 \rightarrow {}^7F_2$) transition of Eu^{3+} ions. There are two groups of emission at 484 nm and 578 nm occurring in the emission spectrum of the ceramics, which probably can be applied for white LEDs application.

Acknowledgement

The authors would like to acknowledge the financial supports from the Fundamental Research Grant Scheme (FRGS) under research grant Project Number: R.J130000.7826.4F140 and the authors would like to thanks Faculty of Science, Universiti Teknologi Malaysia for providing the facilities.

References

[1] Mallawany, R. 1992. The Optical Properties of Tellurite Glasses. *Journal of Appl. Phys*. 72: 1774.

[2] Babu, P., H.J. Seo, K.H. Jang, K.U. Kumar, C.K. Jayasankar. 2007. Optical Spectroscopy, 1.5µm Emission, and Upconversion Properties of Er^{3+}-doped Metaphosphate Laser Glasses. *Chem. Phys. Letter* 445: 162.

[3] Joshi, P., S. Shen, and A. Jha. 2008. Er^{3+}-doped Boro-Tellurite Glass for Optical Amplification in the 1530-1580 nm, *Journal of Appl. Phys.* 103: 083543.

[4] Sudhakar, B. and S. Buddhudu. 2008. Spectral Analysis of Nd^{3+} & Er^{3+}:B_2O_3-(TeO_2/CdO/ZnO)-Li_2O-AlF_3 glasses. *Journal of Optoelectron. Adv. Mater.* 10: 2777–2781.

[5] Rada, S., E. Culea, V. Rus, M. Pica and M. Culea. 2008. The Local Structure of Gadolinium Vanado-Tellurite Glasses. *Journal of Materials Science.* 43: 3713–3716.

[6] Konijnendijk, W.L. and J.M. Stevels. 1975. The Structure of Borate Glass Studied by Raman Scattering. *Journal of Non-Cryst. Solids.* 18: 30.

[7] Bhargava, A.,R.L. Snyder and R.A. Condrate. 1987. The Raman and IR spectroscopy of the Glasses in the System of BaO.TiO_2.B_2O_3. *Mater. Res. Bull.* 22: 1603.

[8] Pascuta, P., L. Pop, S. Rada, M. Bosca, and E. Culea. 2008. The Local Structure of Bismuth Borate Glasses doped with Europium Ions Evidenced by FT-IR Spectroscopy. *Journal of Materials Science Materials in Electronics*. 19: 424–428.

[9] Maheshvaran, K. and K. Marimuthu. 2011. Structural and Optical Investigations on Dy^{3+} doped Boro-Tellurite Glasses. *Journal of Alloys and Compounds*. 509: 7427–7433.

[10] Selvaraju, K., K. Marimuthu, T.K. Seshagiri, S.V. Godbole. 2011. Thermal, Structural and Spectroscopic Investigations on Eu^{3+} doped Boro-Tellurite Glasses. *Journal of Materials Chemistry and Physics* 131: 204–210.

[11] Chen, B.J., E.Y.B. Pun, H. Lin. 2009. Photoluminescence and Spectral Parameters Eu^{3+} in Sodium-Aluminum-Tellurite Ceramics. *Journal of Alloys and Compounds*. 479: 352–356.

[12] Alias, N.S., R. Hussin, M.A. Salim, S.A.A. Fuzi, M. S. Abdullah, S. Abdullah and M. N. M. Yusof. 2009. Structural Studies on Magnesium Calcium Tellurite doped with Eu^{2+} and Dy^{3+}. *Solid State Science and Technology*. 17:50–58.

[13] Bohari, N.Z.I, R. Hussin, Z. Ibrahim, M.H. Haji Jumali, R. Uning and A. Rohaizad. 2014. Structural and luminescence properties of Eu^{3+} and Dy^{3+}-doped Magnesium Boro-Tellurite ceramics. *Advanced Materials Research*. 895: 269–273.

[14] Dwivedi, B.P. and B.N. Khanna. 1995. Cation Dependence of Raman Scattering in Alkali Borate Glasses. *J. Phys. Chem. Solids*. 1: 39–49.

[15] Pavani, P.G., S. Suresh and V.C. Mouli. 2011. Studies on Boro Cadmium Tellurite Glasses, *J. of Optical Materials* 34: 215–220.

[16] Maheshvaran, K., K. Linganna and K. Marimuthu. 2011. Composition Dependent Structural and Optical Properties of Sm^{3+} doped Boro-Tellurite Glasses. *Journal of Luminescence*. 131: 2746–2753.

[17] Rada, S., M. Culea and E. Culea. 2008. Structure of TeO_2.B_2O_3 Glasses Inferred from Infrared Spectroscopy and DFT Calculations. *Journal of Non-Crystalline Solid*. 354: 5491–5495.

[18] Azevedo, J., J. Coelho, G. Hungerford and N.S. Hussain. 2010. Lasing Transition ($^4F_{3/2}\rightarrow{}^4I_{11/2}$) at 1.06µm in Neodymium Oxide doped Lithium Boro Tellurite Glass. *J. of Physica B*. 405: 4696–4701.

[19] Lourenco, S.A., N.O. Dantas, E.O. Serqueira, W.E.F. Ayta, A.A. Andrade, M.C. Filadelpho, J.A. Sampaio, M.J.V. Bell and M.A. Pereira. 2011. Eu^{3+} Photoluminescence Enhancement due to the Thermal Energy Transfer in Eu_2O_3-doped SiO_2-B_2O_3-PbO_2 Glasses System. *Journal of Luminescence*. 131: 850–855.

[20] Lavin, V., P. Babu, C.K. Jayasankar, I.R. Martin and V.D. Rodriguez. 2001. On the Local Structure of Eu^{3+} ions in OxyfluorideGlasses. Comparison with Fluoride and Oxide Glasses. *J. of Chemical Physics*. 115: 10935–10944.

[21] Venkatramu, V., P. Babu and C.K. Jayasankar. 2006. Fluorescence properties of Eu^{3+}ions doped Borate and Fluoroborate Glasses Containing Lithium, Zinc and Lead, *Spectrochimica Acta Part A*. 63: 276–281.

[22] Venkatramu, V., D. Navarro, P. Babu, C.K. Jayasankar, V. Lavin. 2005. Fluorescence Line Narrowing spectral studies of Eu^{3+}-doped Lead Borate Glass. *J. Non-Cryst. Solids*. 351: 929.

[23] Lakshminarayana, G. and J. Qiu. 2008. Photoluminescence of Pr^{3+}, Sm^{3+} and Dy^{3+}:SiO_2–Al_2O_3–LiF–GdF_3 glass Ceramics and Sm^{3+}, Dy^{3+}: GeO_2–B_2O_3–ZnO–LaF_3 Glasses. *Physica B*. 404: 1169–1180.

[24] Lin, Y., Z. Zhang, Z. Tang, X. Wang, J. Zhang and Z. Zheng. 2001. Luminescent Properties of a New Long Afterglow Eu^{3+} and Dy^{3+} Activated $Ca_3MgSi_2O_8$ Phosphor. *Journal of the European Ceramic Society*. 21: 683–685.